

Unimolecular decomposition of chemically activated triplet C_4HD_3 complexes: A combined crossed-beam and ab initio study

R. I. Kaiser^{a)}

Institute of Atomic and Molecular Sciences, 1, Section 4, Roosevelt Rd., 107 Taipei, Taiwan, Republic of China, and Department of Physics, University Chemnitz, Germany and Department of Chemistry, University of York, United Kingdom

A. M. Mebel

Institute of Atomic and Molecular Sciences, 1, Section 4, Roosevelt Rd., 107 Taipei, Taiwan, Republic of China

Y. T. Lee

Institute of Atomic and Molecular Sciences, 1, Section 4, Roosevelt Rd., 107 Taipei, Taiwan, Republic of China

A. H. H. Chang

Department of Chemistry, National Dong Hwa University, Shoufeng, Hualien 974, Taiwan, Republic of China

(Received 21 February 2001; accepted 25 June 2001)

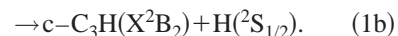
The crossed molecular beam technique was utilized to investigate the reaction of ground state carbon atoms, $C(^3P_j)$, with *d*₃-methylacetylene, $CD_3CCH(X^1A_1)$, at an average collision energy of 21.1 kJ mol⁻¹. Product angular distributions and time-of-flight spectra were recorded. Only the deuterium loss was observed; no atomic hydrogen emission was detected experimentally. Forward-convolution fitting of the data combined with electronic structure calculations show that the reaction is indirect and initiated by a barrierless interaction of the carbon atom to the π -system of the methylacetylene molecule. Reactions with large impact parameters yield a triplet trans-methylpropene-1-diyldene complex whereas—to a minor amount—the formation of a triplet methylcyclopropenylidene intermediate is governed by smaller impact parameters. Both collision complexes rearrange via hydrogen migration and ring opening, respectively, to two distinct triplet methylpropargylene intermediates. A deuterium atom loss via a tight transition state located about 30 kJ mol⁻¹ above the *n*- C_4H_3 product is a likely reaction pathway. The formation of the thermodynamically less stable cyclic isomer remains to be investigated closer. The D atom loss pathway represents an entrance barrierless and exothermic route to synthesize an extremely reactive C_4H_3 hydrocarbon radical in combustion processes and extraterrestrial environments. © 2001 American Institute of Physics. [DOI: 10.1063/1.1394214]

I. INTRODUCTION

Exploring the formation of carbon bearing isomers in hydrocarbon flames and interstellar environments is an important instrument to test chemical models on the evolution of cold molecular clouds, outflow of carbon stars as well as hot molecular cores.¹ Until now, six isomer pairs have been detected in extraterrestrial space, i.e., cyclopropenylidene/vinylidenecarbene, *c*- C_3H_2/H_2CCC , cyclic and linear tricarbonhydride, *c*- $C_3H/1-C_3H$, hydrogen cyanide/hydrogen isocyanide, HCN/HNC, cyanomethane/isocyanomethane, CH_3CN/CH_3NC , magnesium cyanide and isocyanide, MgCN/MgNC and ethyleneoxide/acetaldehyde, *c*- C_2H_4O/CH_3CHO .² Cyanoacetylene/isocyanoacetylene/*N*-butatrienylidene, HCCCN/HCCNC/HNCCC,³ and acetic acid/formic acid methyl ester/glycolaldehyde, $CH_3COOH/$

$HCO_2CH_3/HCOCH_2OH$,⁴ are the only two cases in which three structural isomers have been reported. However, no conclusive evidence has been given if ion-molecule or neutral-neutral reactions form isomers selectively. A better understanding of these elementary processes is therefore necessary.

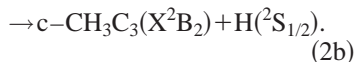
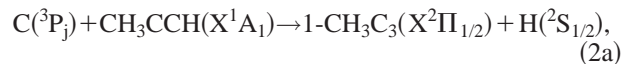
The crucial role of neutral-neutral reactions to synthesize hydrocarbon isomers under controlled reaction conditions was investigated recently in laboratory experiments employing the crossed molecular beams technique.⁵ These studies elucidated the collision energy dependent chemical dynamics of ubiquitous interstellar carbon atoms, $C(^3P_j)$, with acetylene, C_2H_2 to form both astronomically observed linear and cyclic tricarbonhydride isomers:



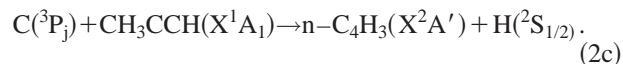
The methyl-substituted counterparts, i.e., the 1- CH_3C_3 and *c*- CH_3C_3 isomers, have never been detected in extraterres-

^{a)}Present address: Department of Chemistry, University of York, York YO10 5DD, UK. Corresponding author. Electronic mail: rikl@york.ac.uk

trial environments. A potential synthetic route might be the reaction of $C(^3P_j)$ with methylacetylene, $CH_3CCH(X^1A_1)$:



Previous crossed-beam studies of this reaction were performed at two collision energies of 20.4 kJ mol^{-1} and 33.2 kJ mol^{-1} . These investigations revealed that the thermodynamically most stable $n-C_4H_3(X^2A')$ was synthesized at the higher collision energy.⁶



The authors suggested, however, that at lower collision energy a hitherto not identified thermodynamically less stable C_4H_3 product was likely to be formed. Therefore, more extensive studies of this reaction are necessary to resolve this open issue.

In the present paper, we address this unanswered question using the following strategy. First, reaction (2) is performed at low collision energy using partially deuterated methylacetylene, CD_3CCH . If channel (2a) or (2b) is open under our experimental conditions, the CD_3 group should be conserved, and only H atom elimination is expected. Second, *ab initio* calculations are performed on the $C(^3P_j) + CH_3CCH$ reaction on the triplet C_4H_4 potential energy surface (PES). Finally, we compare RRKM calculations with our experimental findings.

II. EXPERIMENTAL SETUP

The experiments are carried out under single collision conditions employing the 35" crossed molecular beams machine. The details of the setup are described in Ref. 7. Briefly, a pulsed supersonic carbon beam is generated via laser ablation of graphite at 266 nm.⁸ The 30 Hz, 35–40 mJ output of a Spectra Physics GCR-270-30 Nd:YAG laser is focused onto a rotating carbon rod, and the ablated carbon atoms are seeded into helium released by a pulsed valve operating at 60 Hz, 80 μs pulses, and 4 atm backing pressure. A four-slot chopper wheel mounted 40 mm after the ablation zone selects a 9.0 μs segment of the seeded carbon beam with a peak velocity of $v_p = 1960 \text{ ms}^{-1}$ and speed ratio $S = 7.5$. This beam crosses a pulsed d3-methylacetylene beam, CD_3CCH , with $v_p = 825 \text{ ms}^{-1}$ and $S = 12.3$ at 590 torr backing pressure at 90° in the interaction region of the scattering chamber with a collision energy of 21.2 kJ mol^{-1} . Reactively scattered products are probed in the plane defined by both beams using a triply differentially pumped, rotatable detector. The latter consists of a Brink-type electron-impact ionizer,⁹ quadrupole mass filter, and a Daly ion detector. The velocity distribution of the products is recorded using the time-of-flight (TOF) technique, whereas the laboratory angular distribution (LAB) is obtained by integrating these TOF spectra and correcting for the carbon beam intensity and different data acquisition times at distinct laboratory angles. A forward-convolution routine is used to obtain information on the chemical dynamics of the reaction by fitting the TOF

spectra and the LAB distribution.¹⁰ This procedure initially presupposes an angular flux distribution $T(\theta)$ and a translational energy flux distribution $P(E_T)$ in the center-of-mass system. Hereafter, TOF spectra and the LAB distribution are calculated from these $T(\theta)$ and $P(E_T)$ averaged over the apparatus and beam functions. Best fits of the TOF and laboratory angular distributions are archived by iteratively improving adjustable $T(\theta)$ and $P(E_T)$ parameters. The final outcome results into a velocity flux contour map in the center-of-mass (CM) frame showing the intensity, $I(\theta, u) \sim T(\theta) \times P(u)$, as a function of the angle θ and velocity u in the center-of-mass frame.

III. AB INITIO AND RRKM CALCULATIONS

The geometries of the reactants, products, various intermediates, and transition states for the $C(^3P_j) + CH_3CCH$ reaction were optimized using the hybrid density functional B3LYP method, i.e., Becke's three-parameter nonlocal exchange functional¹¹ with the nonlocal correlation functional of Lee, Yang, and Parr,¹² and the 6-311G(d,p) basis set.¹³ Vibrational frequencies, calculated at the B3LYP/6-311G(d,p) level, were used for a characterization of stationary points, zero-point energy (ZPE) correction, and for the RRKM calculations. All the stationary points were identified for minimum (number of imaginary frequencies NIMAG = 0) or transition state (NIMAG = 1). In some cases, geometries and frequencies were recalculated at the MP2/6-311G(d,p) and CCSD(T)/6-311G(d,p) level.¹⁴ In order to obtain more reliable energies, we used the G2M(RCC,MP2)¹⁵ method, a modification of the GAUSSIAN-2 [G2(MP2)] approach.¹⁶ The GAUSSIAN 94,¹⁷ MOLPRO 96,¹⁸ and ACES-II¹⁹ programs were employed for the potential energy surface computations.

To compare our experimental findings with theoretical predictions, rate constants $k(E)$ at a collision energy E for a unimolecular reaction $A^* \rightarrow A^\ddagger \rightarrow P$ were calculated according to the quasi equilibrium theory or RRKM theory,²⁰ A^* denotes the activated complex, A^\ddagger the transition state, and P the products. As a result, the concentration of each species present in the reaction mechanism was obtained as a function of time. The concentration of the products at $t \rightarrow \infty$ were then taken to calculate branching ratios (cf. Ref. 21 for details).

IV. RESULTS

A. Reactive scattering signal

Reactive scattering signal was observed at mass to charge ratios $m/e = 53, 52, 51, 50, 49$, and 48 , i.e., $C_4D_2H^+$, $C_4D_2^+$, C_4HD^+ , C_4D^+ , C_4H^+ , and C_4^+ (c.f. Figs. 1–3). Time-of-flight spectra at mass to charge ratios 52–48 depicted identical TOF patterns as those spectra recorded at $m/e = 53$. Hence, these lower masses resulted from cracking of the $C_4D_2H^+$ parent ion in the electron impact ionizer of the detector. Compared to the reaction with CH_3CCH , a pronounced shoulder in those TOF spectra close to the center-of-mass angles is evident. This is the result of the mass combination of the products C_4D_2H/D which translates into a broader Newton circle in the deuterated case and increased resolution of the TOF spectra. We like to stress that no signal

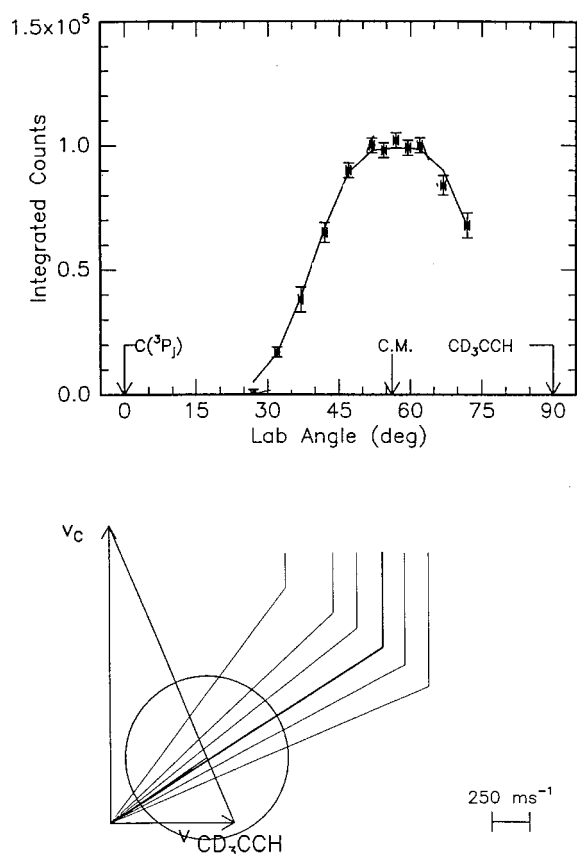


FIG. 1. Lower: Newton diagram for the reaction $C(^3P_1) + CD_3CCH (X^1A_1)$. The circle stands for the maximum center-of-mass recoil velocity of the $n-C_4D_2H$ isomer assuming no energy channels into the internal degrees of freedom. Upper: Laboratory angular distribution of $m/e=52$. Circles and 1σ error bars indicate experimental data, the solid lines the calculated distribution for the C_4D_2H product. C.M. designates the center-of-mass angle. The solid lines originating in the Newton diagram point to distinct laboratory angles whose TOF's are shown in Fig. 2.

of $C_4D_3^+$ at $m/e=54$ was detected. If we account for the data accumulation time and the noise level, the H atom elimination channel shows only an upper limit of $<0.01\%$ relative to the D atom loss pathway. This is a clear indication that the carbon–hydrogen exchange is closed under our experimental conditions; only the atomic carbon versus deuterium exchange is observed. In addition, no radiative association to C_4D_3H ($m/e=55$) could be traced, indicating that internally excited C_4D_3H complex(es) did not survive under our single collision conditions.

B. Laboratory angular distribution (LAB) and TOF spectra

The most probable Newton diagram of the title reaction together with the laboratory angular (LAB) distribution of the C_4D_2H product and TOF spectra are displayed in Figs. 1–3. The TOF spectra at $m/e=52$ and 53 were fit with identical $T(\theta)$ and $P(E_T)$ distributions (cf. Secs. IV.C and IV.D). This strongly supports the conclusion that $m/e=52$ results from cracking of $m/e=53$ in the electron impact ionizer. The LAB distribution peaks at 57.0° close to the CM angle of 56.5° , suggesting that the reaction proceeds through a complex (indirect scattering dynamics) of which its lifetime is

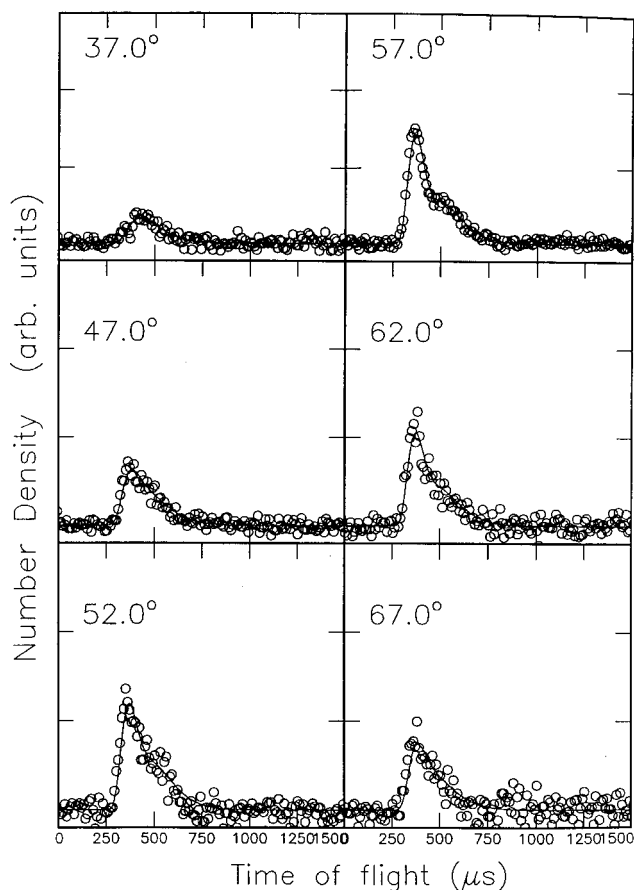


FIG. 2. Time-of-flight data at $m/e=52$ for indicated laboratory angles. Open circles represent experimental data, the solid line the fit. TOF spectra have been normalized to the relative intensity at each angle.

longer than its rotational period. In addition, the reactive scattering signal is spread at least over 50° within the scattering plane. This broad distribution combined with the light D atom proposes a $P(E_T)$ peaking away from zero.

C. Center-of-mass translational energy distribution, $P(E_T)$, center-of-mass angular distribution, $T(\theta)$, and flux contour map $I(\theta, u)$

The best fit of the translational energy distribution $P(E_T)$, the angular distribution $T(\theta)$, and the flux contour map $I(\theta, u)$ are shown in Figs. 4 and 5. Both the LAB distribution and TOF data were fit with a single $P(E_T)$ extending to a maximum translational energy release E_{max} of 120 kJ mol^{-1} . Cutting this tail by up to 30 kJ mol^{-1} does not influence the fits. Likewise adding a long tail up to 200 kJ mol^{-1} with an intensity of 0.01 – 0.015 relative to the distribution maxima of the $P(E_T)$ results in an identical fit. In addition, the $P(E_T)$ peaks away from zero as expected from the LAB distribution and reveals a broad plateau between 25 – 35 kJ mol^{-1} . Finally, the total average available energy channeling into the translational degrees of the reaction products is 40 – 42 kJ mol^{-1} .

Both the $T(\theta)$ and $I(\theta, u)$ distributions are symmetric around $\pi/2$ (c.f. Figs. 4 and 5). This implies that either the lifetime of the decomposing C_4D_3H complex is longer than

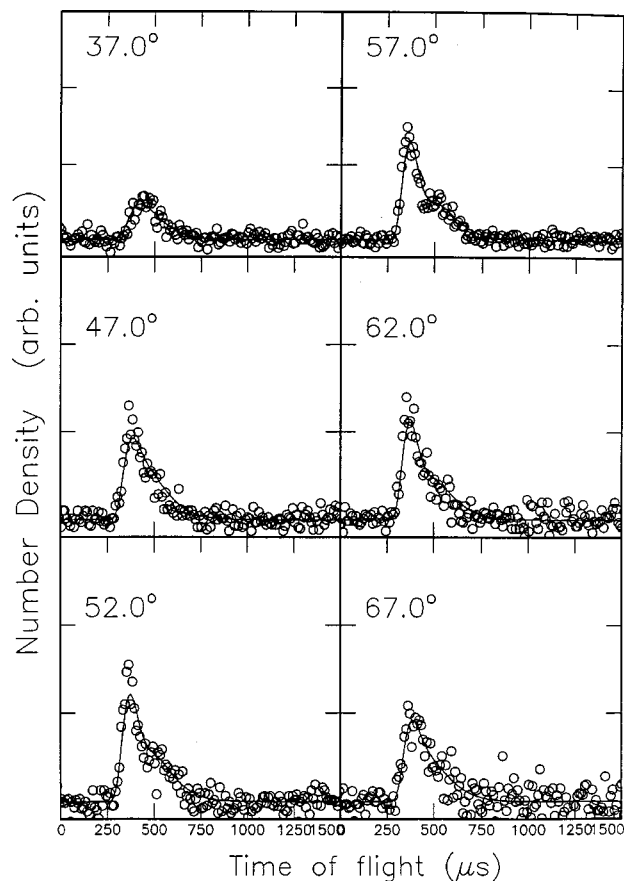


FIG. 3. Time-of-flight data at $m/e=53$ for indicated laboratory angles. Open circles represent experimental data, the solid line the fit. TOF spectra have been normalized to the relative intensity at each angle.

its rotational period τ_r or that two deuterium atoms of the intermediate can be interconverted through a rotational axis.²² In this case, the light D-atom could be emitted in θ and $\theta-\pi$ to result for the forward-backward symmetry of $T(\theta)$. The flat angular distribution results from a weak coupling between the initial and final angular momentum vectors, \mathbf{L} and \mathbf{L}' , respectively. Since bulk experiments, as well as a crossed-beam investigation, suggest that the reaction of atomic carbon with methylacetylene proceeds without entrance barrier within orbiting limits,²³ we approximate the maximum impact parameter b_{\max} to be 3.7 \AA at our collision energy of 21.2 kJ mol^{-1} .⁶

V. DISCUSSION

A. The C_4H_4 potential energy surface

In the following section, we discuss possible reaction pathways based on our *ab initio* calculations on the $C(^3P_j)+CH_3CCH$ reaction. Although our experiments were performed with CD_3CCH and not with CH_3CCH , the energetics of the intermediates and products change only slightly by $1\text{--}2 \text{ kJ mol}^{-1}$ due to the difference in zero point vibrational energy. For a complete description of the PES we refer to Ref. 24. Here, only those results necessary to understand the experimental findings are presented. We refer to the carbon atom adjacent to the acetylenic hydrogen as C1, the central one as C2, and the methyl carbon atom as C3.

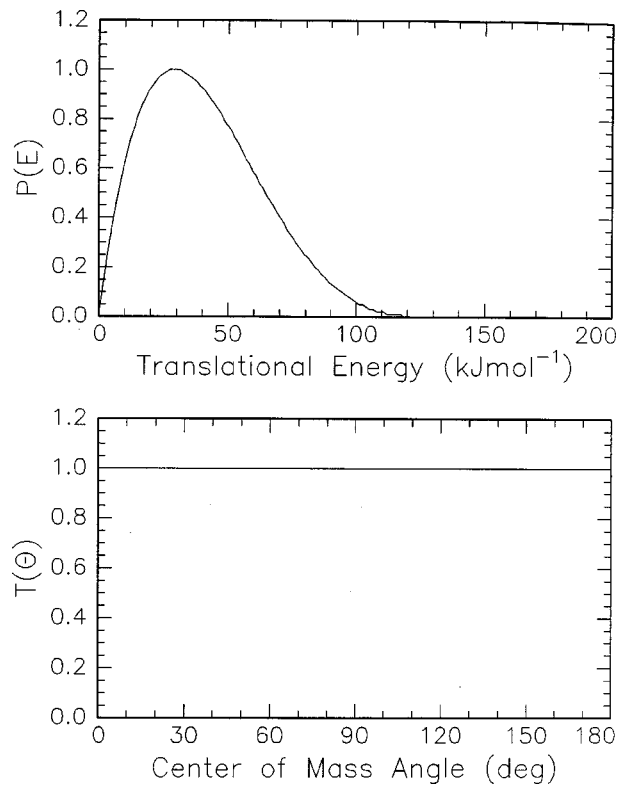


FIG. 4. Center-of-mass translational energies flux distribution for the reaction $C(^3P_j)+CD_3CCH(X^1A_1)\rightarrow C_4D_2H+D(^2S_{1/2})$. The solid line limits the range of acceptable fits within 1σ error bars.

Our electronic structure calculations show that $C(^3P_j)$ can interact with methylacetylene on the triplet surface via four barrierless entrance channels. First, the carbon atom can add to the C2 carbon atom to form trans- and cis-methylpropene-2-diylidene (**i1** and **i2**, respectively), as shown in Figs. 6 and 7. An attack on the C1 position leads to trans-methylpropene-1-diylidene (**i3**); a cis isomer of **i3** was found not to be a local minimum. Since these isomers are bound by 124.7 , 116.3 , and $136.8 \text{ kJ mol}^{-1}$ with respect to the reactants, the rotational barrier of the CH_3 group of about 10.5 kJ mol^{-1} can be overcome easily; this results in a C_s point group and $^3A''$ electronic wave function of **i1**, **i2**, and **i3**. The remaining pathway involves an addition of $C(^3P_j)$ to both the C1 and C2 to form triplet methylcyclopropenyliidene, **i4**. This isomer has no symmetry element and is stabilized by $220.9 \text{ kJ mol}^{-1}$ compared to $C(^3P_j)$ and CH_3CCH . All three methylpropenediylidene isomers can undergo ring closures to **i4** via transition states located $10\text{--}18 \text{ kJ mol}^{-1}$ higher than **i1**–**i3**. In **i3**, this pathway competes with a hydrogen 2,1-H shift. A small barrier of only 0.8 kJ mol^{-1} separates the latter from triplet methylpropargylene (**i5**), belongs to the C_1 point group and has a 3A electronic wave function. The floppiness of this molecule is documented by two low frequency bending modes of the terminal carbon–hydrogen (33 cm^{-1}) and the terminal carbon–carbon bond (200 cm^{-1}). Under our experimental conditions, both bending modes can be excited, and the methyl group rotates freely. This results in a quasilinear arrangement of all carbon atoms and a C_{3v}

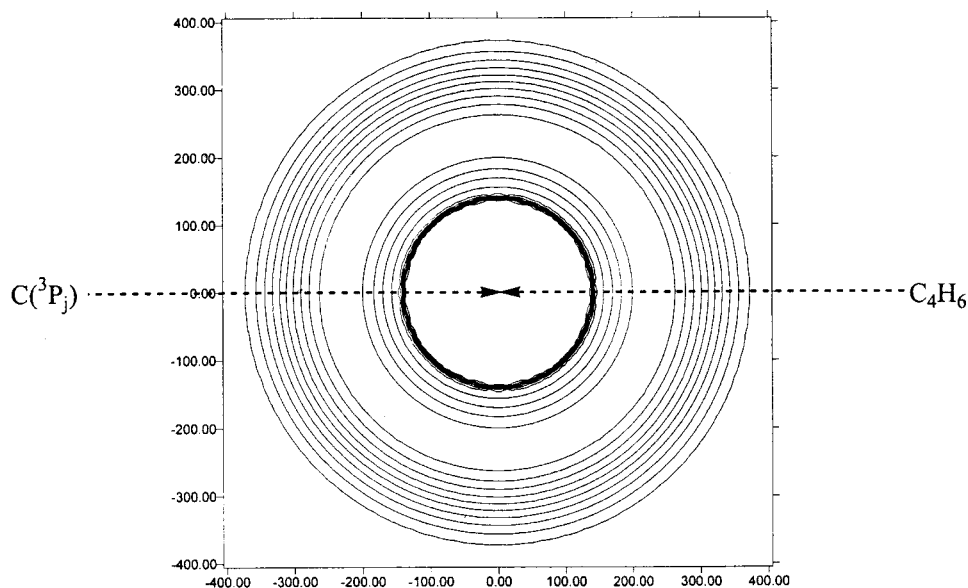


FIG. 5. Contour flux map for the reaction $C(^3P_j) + CD_3CCH (X^1A_1) \rightarrow C_4D_2H + D(^2S_{1/2})$ depicting the velocity of the $n-C_4D_2H$ products in the CM frame; units are given in ms^{-1} .

point group of **i5**. Further, a ring opening of **i4** can lead to **i5** via a barrier of 61.5 kJ mol^{-1} . The intermediate **i6** (triplet buten-3-yne-1) can be formed through a 3,2 hydrogen atom shift from triplet methylpropargylene.

B. The C_4H_3 potential energy surface

Figure 7 depicts the equilibrium structures of three potentially involved doublet C_4H_3 reaction products. The $n-C_4H_3$ (**p1**) isomer represents the global minimum of the C_4H_3 potential energy surface. It belongs to the C_s point group and has a $^2A'$ electronic wave function. Its ground state is a bent structure, whereas the linear structure represents a transition state between two bent states, located only 3.1 kJ mol^{-1} above the $n-C_4H_3$. Via C–H bond ruptures of **i5** and **i6** via tight exit transition states located $24\text{--}30 \text{ kJ mol}^{-1}$ above the separated products, **p1** can be formed.

Compared to the n -isomer, $i-C_4H_3$ (**p2**) is energetically less favored by 45.6 kJ mol^{-1} . In addition, **p2** has the same point group and electronic wave function as **p1** and can be formed through carbon–hydrogen cleavage of **i6**. The cyclic structure **p3** is less stable by $123.8 \text{ kJ mol}^{-1}$ compared to $n-C_4H_3$; a hydrogen atom emission from **i4** is the sole pathway to this isomer.

C. Identification of reaction product(s)

Our center-of-mass translational energy distribution, $P(E_T)$, demonstrates that the reaction of atomic carbon with methylacetylene is exothermic by at least $70\text{--}100 \text{ kJ mol}^{-1}$. Since a long tail could justify exothermicity up to 180 kJ mol^{-1} , the computed reaction energies to form **p1**, **p2**, and **p3** suggest that the thermodynamically most stable $n-C_4H_3$ isomer **p1** presents part of the reaction products. The calcu-

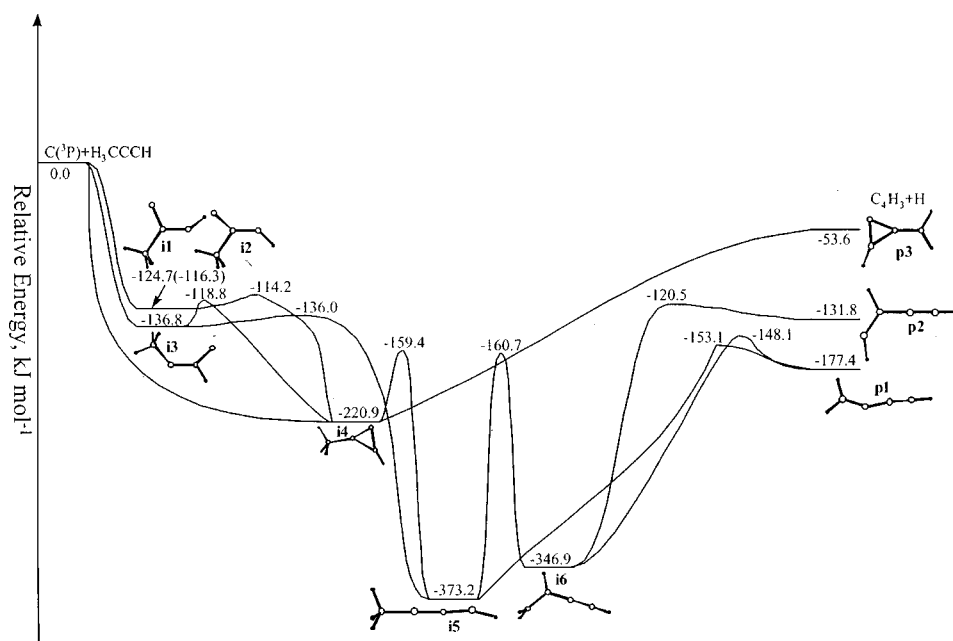


FIG. 6. Schematic representation of the lowest energy pathways on the triplet C_4H_4 PES and structures of potentially involved collision complexes for the $C(^3P_j) + CH_3CCH (X^1A_1)$ reaction. Those structures designated with “i” indicate intermediates, those with “p” potential C_4H_3 isomers.

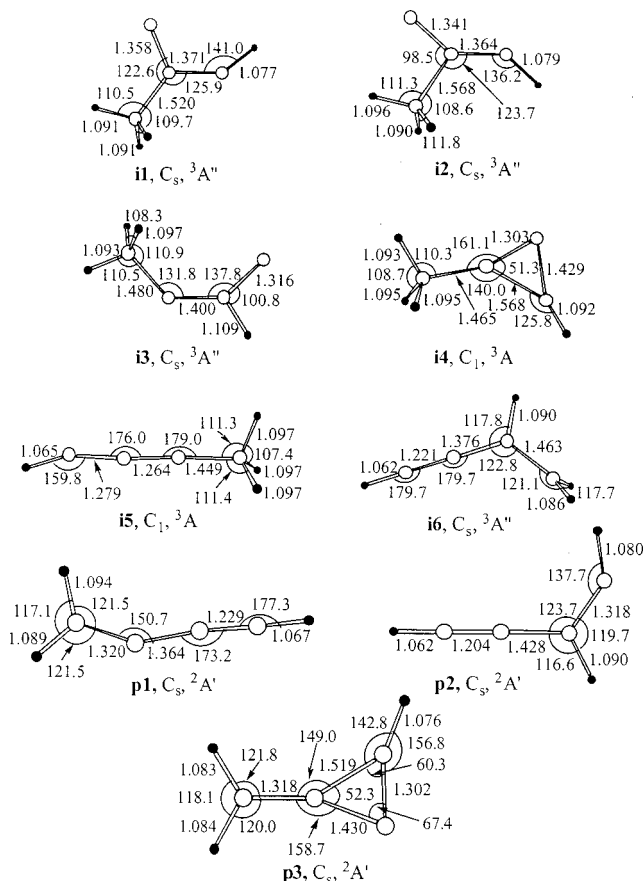


FIG. 7. Structures of potentially involved triplet C_4H_4 collision complexes and products. Important bond lengths are given in Angstrom, bond angles in degrees. Those structures designated with “i” indicate intermediates, those with “p” potential C_4H_3 isomers.

lated data of $-177.4 \text{ kJ mol}^{-1}$ is in good agreement with the crossed beam results. Even accounting for the less exothermic reaction to the iso C_4H_3 product, **p2** cannot explain the experimentally determined data of $70\text{--}100 \text{ kJ mol}^{-1}$ alone. Based on the energetics of **p3**, we would expect an exothermicity of about 54 kJ mol^{-1} , which could explain only the part of the $P(E_T)$ toward lower translational energies. Summarized, these findings suggest formation of the thermodynamically most stable product **p1** and possibly fractions of **p2** and/or **p3**. As evident from the $P(E_T)$, the exothermicity to form **p1**+D is partitioned into rotation and vibrational energy of the $n\text{-}C_4H_3$ product.

Our results correlate nicely with the crossed-beam observation of the carbon versus deuterium exchange pathway. Here, the D atom can only originate from the d3-methyl group but not from the acetylenic carbon–hydrogen bond. As evident from the involved potential energy surface (Fig. 6), a deuterium release verifies formation of **p1** (from **i5** and/or **i6**), **p2** (from **i6**), and/or **p3** (from **i4**). Reactions (2a) and (2b) to methyl substituted tricarbon hydride molecules, $CCCD_3$ and $c\text{-}C_3CD_3$, were not observed since a hydrogen atom loss from **i5** and **i4** would have been required. This was clearly not observed experimentally.

These findings can be compared with microcanonical transition state calculations. Since RRKM theory can be applied only for unimolecular reactions, we cannot calculate

TABLE I. Calculated RRKM rate constants (s^{-1}) for various reaction steps.

$k_{i1 \rightarrow i4}$	1.34×10^{12}
$k_{i1 \rightarrow i4}$	8.51×10^{10}
$k_{i3 \rightarrow i4}$	5.69×10^{12}
$k_{i3 \rightarrow i4}$	2.40×10^{11}
$k_{i3 \rightarrow i5}$	5.76×10^{13}
$k_{i3 \rightarrow i5}$	1.20×10^8
$k_{i4 \rightarrow i5}$	4.37×10^{12}
$k_{i4 \rightarrow i5}$	2.16×10^8
$k_{i4 \rightarrow i3}$	2.90×10^{10}
$k_{i5 \rightarrow i6}$	6.84×10^9
$k_{i5 \rightarrow i6}$	3.63×10^{10}
$k_{i5 \rightarrow p1}$	1.34×10^9
$k_{i6 \rightarrow p1}$	1.93×10^{10}
$k_{i6 \rightarrow p2}$	2.40×10^9

the branching ratio for the attack of atomic carbon to C1, C2, or C1 plus C2 of the methylacetylene molecule. To avoid this problem, the resulting branching ratios for **p1**, **p2**, and **p3** were expressed as a function of **i1**–**i4** initial concentrations, which were not known. The computed branching ratios were obtained then by plugging in the assumed composition between the initial concentrations of **i1**–**i4**. We assumed that **i1** and **i2** can freely interconvert to each other and considered the following initial concentration ratios of (**i1**+**i2**)/**i3**/**i4**: 1/0/0, 0/1/0, 0/0/1, and 1/1/1 (see Tables I–II). The results for all four cases are similar and suggest that the formation of **p1** should contribute 90–91% to the products; **p2** and **p3** are found to be of minor importance and provide only 9–10% (**p2**) and less than 1% (**p3**).

D. The actual reaction pathway

The reaction pathway and chemical reaction dynamics are discussed in terms of different approach geometries of the carbon atom towards the methylacetylene molecule. Although our crossed-beam data are actually an average over all reactive impact parameters, the following discussion helps to understand the impact parameter dependent formation of distinct collision complexes, the rotational excitation, and the (non)statistical decomposition(s) of distinct intermediates. Our findings suggest that the reaction proceeds via addition of $C(^3P_i)$ to the carbon–carbon triple bond of the methylacetylene molecule. Since the reaction is barrierless and dominated by long-range dispersion forces, primarily large impact parameters are proposed to form the initial collision complex. Considering trajectories with large impact parameters, intermediate **i3** is likely to be formed via an

TABLE II. Calculated product yields at different initial concentrations (**i1**+**i2**)/**i3**/**i4**.

Initial concentration (i1 + i2)/ i3 / i4	p1	p2	p3
1/0/0	0.899	0.0953	0.0054
0/1/0	0.907	0.0922	0.00093
0/0/1	0.902	0.0917	0.0066
1/1/1	0.903	0.0931	0.0043

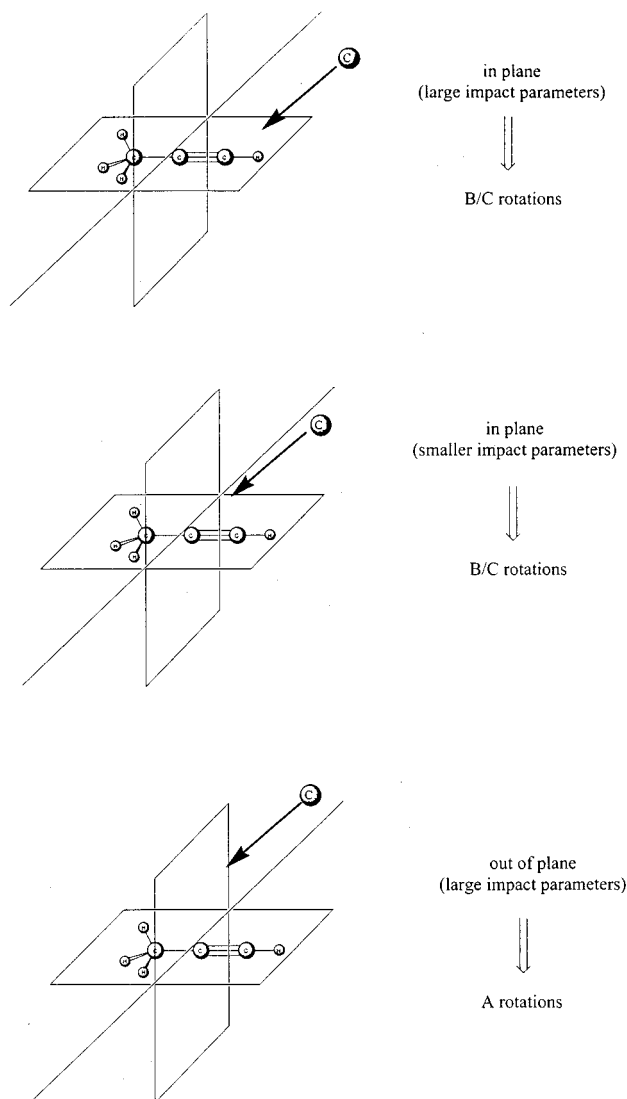


FIG. 8. Schematic representation of distinct approach geometries of atomic carbon towards methylacetylene.

in-plane interaction of both singly occupied p_x and p_y orbitals of $C(^3P_j)$ with two perpendicular π orbitals at C1 [cf. Fig. 8 (*sideways attack*)]. This pathway conserves C_s symmetry, proceeds on the $^3A''$ surface,²⁵ and excites the prolate intermediate **i3** to B- and C-like rotations (Fig. 9). The preferential attack of C1 is supported further by an enhanced electron density of the C1 atom ($-0.14 e$) as compared to that of C2 ($-0.11 e$) due to the π -group orbitals of the methyl substituent (Fig. 10) and the screening effect of the CH_3 group (sterical hindrance), thus reducing the cone of acceptance at C2. Alternatively, large impact parameters could lead via addition of $C(^3P_j)$ to C1 and C2 to the cyclic intermediate **i4**, which rings open to **i5** (*cyclic attack*). This pathway excites rotations of **i5** around its A axis. However, since detailed considerations of energy and angular momentum conservation demonstrated clearly that **i5** can rotate only around the B/C axes,⁶ large impact parameter *dominated cyclic attacks* can be likely ruled out. In strong contrast, approaching smaller impact parameters, atomic carbon interacts closer to the center-of-mass of the methylacetylene molecule (*central*

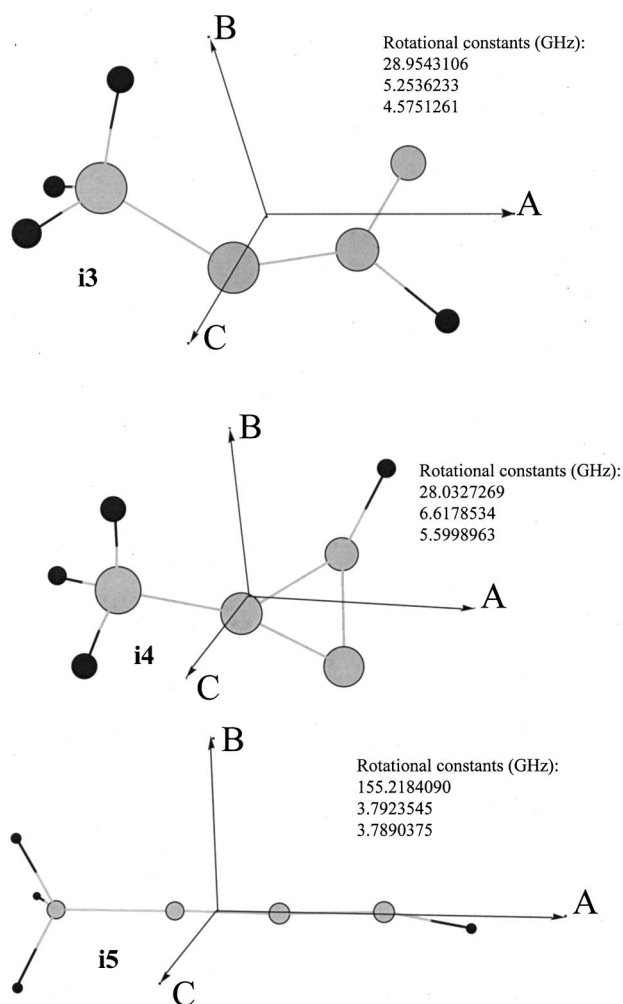


FIG. 9. Principal rotational axes of **i3**, **i4**, and **i5**.

attack). This pathway is expected to form predominantly **i4** and to a smaller amount **i1**/**i2**. Summarized, the formation of **i3** is dominated by large impact parameters, whereas a smaller impact parameters yields the cyclic intermediate **i4**. Trajectories with impact parameters close to zero are expected to yield **i1** and **i2**. But due to the overwhelming contribution of large impact parameters and the directing effect of the methyl group, addition to C2 is expected to be only of minor importance.

But what is the fate of the initial collision complexes? To form **i4**, **i1** and **i2** undergo ring closure. Since the barrier of a

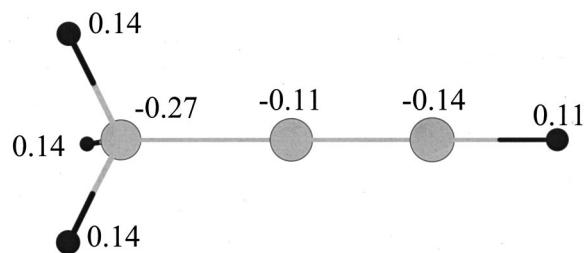


FIG. 10. Charge densities in the methylacetylene reactant derived from the population analysis.

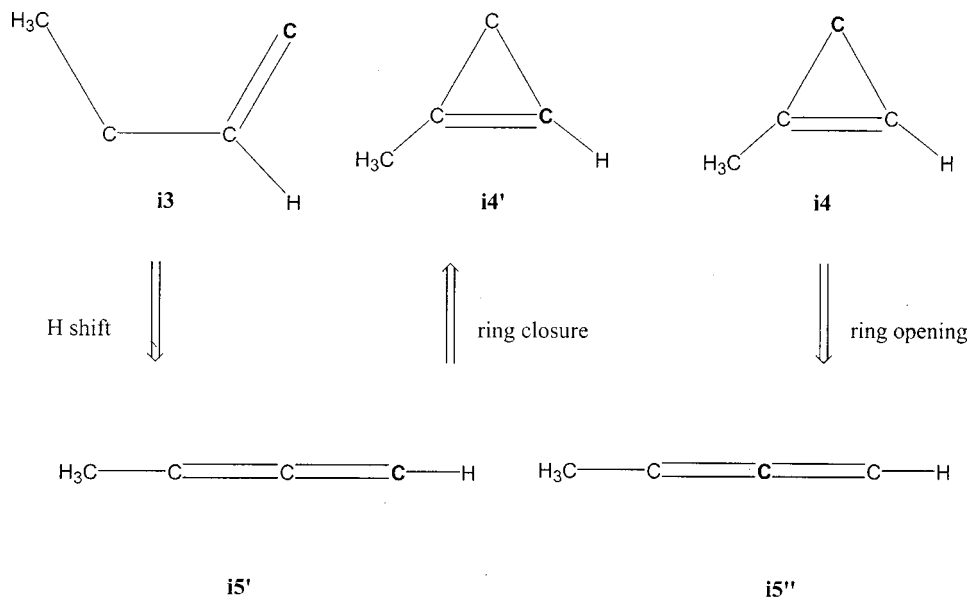


FIG. 11. Schematic pathways to the triplet methylpropargylene intermediate via hydrogen migration (left; **i5'**) and ring opening (right, **i5''**) together with ring closure to **i4'**. The reacting atom is displayed in bold.

2,1-H shift in **i3** is only 0.8 kJ mol^{-1} , we expect that **i3** reacts via hydrogen migration to methylpropargylene, **i5**, rather than undergoing a ring closure to **i4** (Fig. 11). A second route to **i5** involves a ring opening of **i4**. Although both mechanisms lead to methylpropargylene, the complexes formed are not equivalent since the carbon atom is formally inserted into the C1-H bond (**i5'**) or into the C1-C2 bond (**i5''**) (Fig. 11). Via a tight exit transition state to the $n\text{-C}_4\text{H}_3$ isomer **p1** and atomic deuterium, **i5'** and **i5''** decompose. This is well-reflected in a $P(E_T)$ peaking away from zero translational energy. However, we would like to stress that both **i5** complexes might have different life times prior to their fragmentation. This has to be investigated further.

VI. CONCLUSIONS

The crossed molecular beam technique was employed to study the reaction of ground state carbon atoms, $\text{C}(P_j)$, with d3-methylacetylene, $\text{CD}_3\text{CCH}(X^1A_1)$, at a relative collision energy of 21.1 kJ mol^{-1} . Combining the experimental data with electronic structure calculations, the reaction is found to be indirect and initiated by a barrierless interaction of the carbon atom to the π -system of the methylacetylene molecule. Large impact parameters could yield a triplet trans-methylpropene-1-diyldene complex **i3**, whereas the formation of a triplet methylcyclopropenyldene complex **i4** is dictated by small impact parameters close to zero. The intermediates **i3** and **i4** are excited to B/C-like rotations, rearrange via hydrogen migration, and ring open to two distinct triplet methylpropargylene complexes (**i5'** and **i5''**). In this picture, the data can be explained assuming the methylpropargylene intermediates decompose via D atom loss to the $n\text{-C}_4\text{H}_3$ isomer. This explicit assignment of the carbon versus deuterium exchange and identification of a tetracarbon-trihydride isomers under single collision conditions, employing the universal crossed beams machine, demonstrates explicitly the great advantage compared to a previous study detecting the light hydrogen atom via one-photon resonant laser induced fluorescence.²³ Although Chastaing *et al.* deter-

mined integral cross sections, the identification of the C_4H_3 products isomer(s) failed. Since the optical properties and resonant as well as nonresonant detection schemes of C_4H_3 isomers are presently unknown, an explicit identification of the product isomers is not feasible and relies—as the authors state themselves—on data obtained from universal crossed-beam machines. Our findings have further strong implications to model chemical processes in the interstellar medium and combustion flames, including distinct structural isomers into sophisticated reaction networks.

ACKNOWLEDGMENTS

One of the authors (R.I.K.) is indebted to the Deutsche Forschungsgemeinschaft for a *Habilitation* fellowship (IIC1-Ka1081/3-1). The data accumulation was further financed by Academia Sinica, Taiwan. Data analyses and preparation of this publication was supported by Department of Chemistry, University of York, UK. This work was performed within the *International Astrophysics Network*.

¹E. Herbst, H. H. Lee, D. A. Howe, and T. J. Millar, *Mon. Not. R. Astron. Soc.* **268**, 335 (1994).

²J. E. Dickens *et al.*, *Ap. J.* **489**, 753 (1997).

³Y. Osamura, K. Fukuzawa, R. Terzieva, and E. Herbst, *Ap. J.* **519**, 697 (1999).

⁴J. M. Hollis, F. J. Lovas, and P. R. Jewell, *Ap. J.* **540**, L107 (2000).

⁵R. I. Kaiser, C. Ochsenfeld, M. Head-Gordon, Y. T. Lee, and A. G. Suits, *J. Chem. Phys.* **106**, 1729 (1997); R. I. Kaiser, C. Ochsenfeld, M. Head-Gordon, Y. T. Lee, and A. G. Suits, *Science* **274**, 1508 (1996).

⁶R. I. Kaiser, D. Stranges, Y. T. Lee, and A. G. Suits, *J. Chem. Phys.* **105**, 8721 (1996).

⁷N. Balucani, O. Asvany, A. H. H. Chang *et al.*, *J. Chem. Phys.* **111**, 7457 (1999).

⁸R. I. Kaiser and A. G. Suits, *Rev. Sci. Instrum.* **66**, 5405 (1995).

⁹G. O. Brink, *Rev. Sci. Instrum.* **37**, 857 (1966).

¹⁰M. S. Weis, Ph.D. thesis, University of California, Berkeley (1986); M. Vernon, thesis, University of California, Berkeley (1981).

¹¹A. D. Becke, *J. Chem. Phys.* **97**, 9173 (1992).

¹²C. Lee, W. Yang, and R. G. Parr, *Phys. Rev. B* **37**, 785 (1988).

¹³R. Krishnan, M. Frisch, and J. A. Pople, *J. Chem. Phys.* **72**, 4244 (1988).

¹⁴G. D. Purvis and R. J. Bartlett, *J. Chem. Phys.* **76**, 1910 (1982).

- ¹⁵A. M. Mebel, K. Morokuma, and M. C. Lin, *J. Chem. Phys.* **103**, 7414 (1995).
- ¹⁶L. A. Curtiss, K. Raghavachari, and J. A. Pople, *J. Chem. Phys.* **98**, 1293 (1993).
- ¹⁷M. J. Frisch, G. W. Trucks, H. B. Schlegel *et al.*, GAUSSIAN 94, Revision D.4 (Gaussian, Inc., Pittsburgh, 1995).
- ¹⁸MOLPRO is a package of *ab initio* programs written by H.-J. Werner and P. J. Knowles, with contributions from J. Almlöf, R. D. Amos, M. J. O. Deegan, S. T. Elbert, C. Hampel, W. Meyer, K. Peterson, R. Pitzer, A. J. Stone, P. R. Taylor, and R. Lindh.
- ¹⁹J. F. Stanton, J. Gauss, J. D. Watts, W. J. Lauderdale, and R. J. Bartlett, ACES-II (University of Florida, FL).
- ²⁰H. Eyring, S. H. Lin, and S. M. Lin, *Basic Chemical Kinetics* (Wiley, New York, 1980).
- ²¹A. H. H. Chang, A. M. Mebel, X. M. Yang, S. H. Lin, and Y. T. Lee, *J. Chem. Phys.* **109**, 2748 (1998).
- ²²W. B. Miller, S. A. Safron, and D. R. Herschbach, *Discuss. Faraday Soc.* **44**, 108, 291 (1967).
- ²³D. Chastaing, S. D. LePicard, I. R. Sims, I. W. M. Smith, W. D. Geppert, C. Naulin, and M. Costes, *Chem. Phys. Lett.* **331**, 170 (2000).
- ²⁴A. M. Mebel, R. I. Kaiser, and Y. T. Lee, *J. Am. Chem. Soc.* **122**, 1776 (2000); A. M. Mebel and R. I. Kaiser, *Angew. Chem. Int. Ed. Engl.* (in preparation).
- ²⁵This point group is assigned since under our experimental conditions; the methyl group rotates freely.